University of Utrecht

Debye Institute

Atom Optics & Ultrafast Dynamics

Measuring the Enhanced Scattering Rate in a Bose-Einstein condensate

Author:
Rens Pieter de Haas

Supervisors:
prof. dr. P. van der Straten
P.C. Bons MSc

June 18, 2014

Abstract

In this thesis we measure and calculate the enhanced scattering rate for both cold thermal clouds and Bose-Einstein condensates. For Bose-Einstein condensates we find that the scattering rate is enhanced, due to the large densities and a temperature just below the critical temperature. The enhancement under typical experimental conditions with a Bose-Einstein condensate is up to a factor 3, while there is no enhancement for thermal clouds. The scattering rate influences both the number of particles and the average energy per particle. For both the energy and the number of particles a theoretical prediction is compared with an experimental result. For the number of particles in a cloud both with and without a Bose-Einstein condensate and the energy in a cloud without a Bose-Einstein condensate, we find that theory and experiment agree within their uncertainties. In the case of the energy per particle in a cloud with a Bose-Einstein condensate, we included a cooling effect for condensed atoms that become thermal, however our experimental results are not sufficient to confirm this theory.

Contents

1 Introduction to making images of a BEC

If light propagates through a medium, some light will be absorbed and re-emitted in a random direction direction (called scattering), and other light will pass through the medium (called transmission). Most of the light seen in every day life has been scattered. Light from a source like the sun or a lamp falls on a surface (an object like a hand) and scatters in every direction including your eyes. Transmitted light is the light coming directly from the source, without any scattering. Since the scattered light is re-emitted in a random direction, the light spreads over an area and the intensity of the light is reduced. Figure 1a gives a schematic view of the situation. The amplitude of the waves of the light corresponds to the intensity of the light.

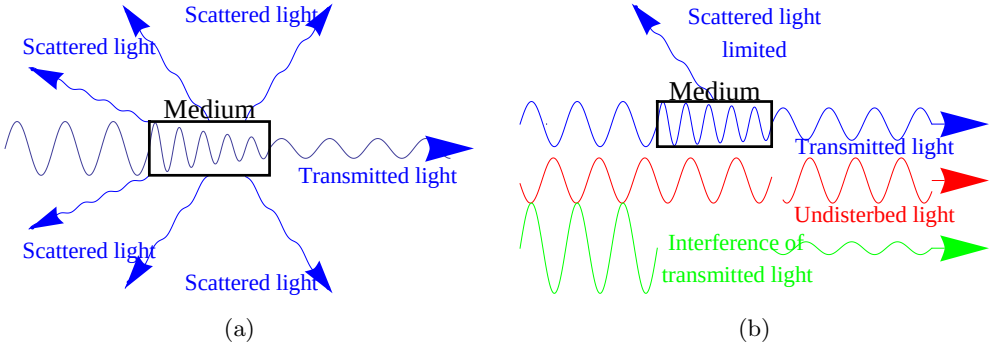

Figure 1: Schematic image of light passing through a medium. (a) Schematic scheme of absorption imaging, some light is absorbed by the medium. When a image is taken of the transmitted light, it is called absorption imaging. When a image is taken of the scattered light, it is called fluoresence imaging. (b) Schematic scheme of phase contrast imaging (PCI), only a minimal amount of light is absorbed by the medium, but the light that passes through the medium gets a phase shift and the light will interfere with undisturbed light. The undisturbed light gets an additional phase shift.

Figure 2 shows different pictures of a hand, where Figure 2a shows the image taken of the scattered light. This is 'everyday-life': anyone could take this picture with their camera or cellphone. Figure 2b shows the transmitted light. This technique is called absorption imaging because the absorption is the negative of the transmission. The amount of scattering and transmission depend on the medium (structure and density) and the light (wavelength). For example, if one would use x-rays, one would also get an insight of the hand as seen in Figure 2c, using the same absorption imaging technique. The amount of transmission depends on whether the light passes through a bone or not. Now some characteristic of the atoms used are discussed before a new imaging technique is introduced.

A Bose-Einstein condensate (BEC) consists of atoms that have a negligible amount of energy compared to a thermal cloud and have an extremely low temperature. If scattered light illuminates a BEC, the BEC will gain energy, thereby increasing the temperature

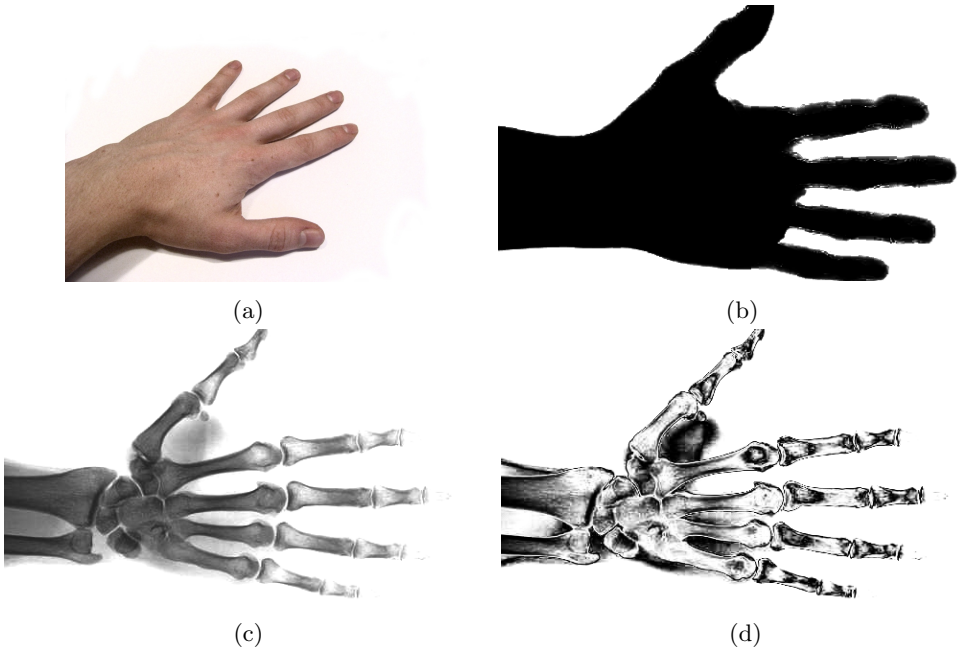

Figure 2: Examples of different kinds of images taken of a hand. (a): Everyday-life imaging, of scattered light.(b): Absorption imaging, of light not scattered. (c): X-ray absorption imaging, of light not scattered. (d): Phase Contrast Imaging.

and particles will be lost. So light which is scattered on a BEC can destroy the BEC. Light which is not scattered will pass through the BEC (like a clear glass window). Light is needed to make a picture, so using the previously described techniques, will either destroy the BEC or result into no picture. If a BEC is destroyed, a new BEC can be made, however it is impossible to make multiple pictures of one single BEC. This limits our ability to detect fast dynamics in the condensate.

For purposes like imaging the dynamics of the BEC, multiple pictures of one single BEC are needed. To prevent the destruction of the BEC, the light shouldn't be scattered, so light that doesn't scatter is used. However some contrast is needed depending on the medium the light travels through (unlike a clear glass window). To overcome this problem, light is also sent around the medium, so it is undisturbed. This light will interfere with the light that has gone through the medium. Since the medium has slowed the light down, the undisturbed light wave will be ahead of the light wave which went through the medium. This causes a phase shift. A schematic view is visible in Figure 1b. The intensity of the interfered light depends on the phase shift which depends on the medium, though a phase shift of exactly a integer of periods won't be noticed. This technique is called Phase Contrast Imaging (PCI).

In Figure 2d it is shown how a hand could look like using PCI. Compare it with the x-ray image in Figure 2c and notice that some of the darker areas of the x-ray image are

white again, while the darkest area of the x-ray are again dark (in the bone of the arm). This is because the delayed light is exactly a period behind. So in a PCI image, the same color can represent different kinds of medium while in absorption the same color implies the same (similar) kinds of medium. The difference for the medium is that no light is scattered.

The typical maximum densities of a BEC is over a factor 10 000 smaller than the density of air. The condensates are cigar-shaped with a length up to one millimeter and a diameter of tens of micrometers. In everyday life the effects of the air between our eyes and a lamp is barely noticed. Notice that the dimensions and density of the condensate are far less than those of the air which causes a barely noticeable effect. So will have very limited contrast. To overcome this problem resonant and near resonant light are used. This light has a large phase shift and a large probability to get scattered.

Kramers-Kronig relations say that probability of a photon to get scattered and the reduction in speed are correlated. So a balance is needed for a small scattering effect and a large phase shift. Atoms have different internal energy levels (ignoring the kinetic and potential energy of the atom). Those levels are quantized, which means that the atom can only have some discrete amounts of energy. If light, with exactly the energy difference between two of these energy levels passes through these atoms, the atoms and the light are likely to interact, causing a large phase shift and a large probability of scattering. This light is called *resonant light*.

Resonant light is used for absorption imaging since this light interacts with the atoms. The energy of resonant light is noted as $\Delta E = E_1 - E_0$ and the corresponding frequency is noted as $\omega = \Delta E/\hbar$. A schematic view of two energy levels is shown in Figure 3a.

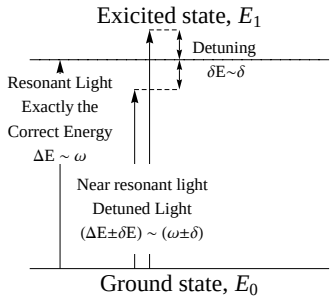

(a) Schematic scheme of two energy levels of an atom. The energy difference between the two levels is ΔE. Near resonant light has an energy of $\Delta E \pm \delta E$ where $\delta E = \delta\hbar$ the detuning is.

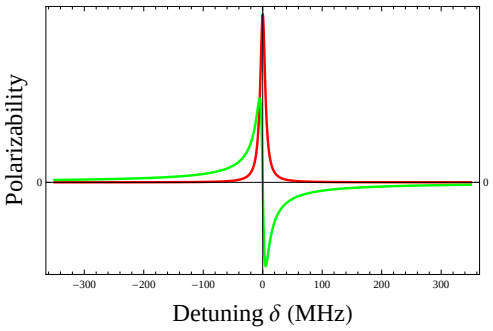

(b) The polarizability of sodium in arbitrary units. Green corresponds with the real part, corresponding the speed reduction. Red corresponds with the imaginary part, corresponding with the scattering.

Figure 3

If the energy of the light is different, the energy and frequency are *detuned*, the energy is

$\Delta E \pm \delta E$, which is not exactly the energy difference of the two levels. Now the scattering probability is reduced but also the phase shift. This is called *near resonance light*. For PCI, near resonance light with a detuning of 0.000068% (=346Mhz) in the energy of the light is used, so that the probability of scattering is reduced with approximately a factor $\frac{1}{5000}$. The scattering rates corresponds with the imaginary part of the polarizability, shown in Figure 3b. If the detuning is larger, the effects of the medium on the light are smaller. This is the reason why the light of the sun (with an energy that isn't selected to be near resonance) travels through the air with a barely noticeable effect.

A few more notes on this introduction. First notice that in this introduction two different kinds of light are pointed out. The main difference of visible light and x-rays is the energy. However in our experiment we use only different variations of resonant light (with almost the same energy), but a different detuning, so these variation have the same color for the human eye . Secondly, notice that the condensate is created in vacuum, since it would heat up and be destroyed if it would get into contact with air. This means that the achieved densities -even though a factor 10 000 smaller than the density of air-, are still relatively large. Furthermore notice that for the use the interference in PCI monochromatic coherent light is needed, which is provided by a laser.

It is possible to make images of Bose-Einstein condensates. When absorption imaging is used, there is a lot of interaction between the atoms and the light, causing the atoms to heat up and to lose all the particles. When phase contrast imaging is used, there limited interaction, causing the system to heat up and to lose a fraction of the particles. In this research I will explain why the system heats and the particles are lost the way they are. I will distinguish between a cold thermal gas, analogue to the Bachelor Thesis of Damaz de Jong [1] and a case where the probability that a single light-photon will interact with one single atom depends on the surrounding atoms. My experimental results are similar to those of Damaz de Jong, though my theoretical description has more effects included.

2 Experimental setup

2.1 Creating a cold cloud

Here I describe very briefly the cooling steps to get an ultra cold cloud. In our experiment a cold thermal cloud is first created. The atoms started in a warm cloud (600K) in the oven in a vacuum chamber. With the use of diaphragms, particles escape in a collimated beam into a *Zeeman slower*, where the particles velocity is reduced. Next the particles are trapped in the Magneto-Optical Trap (MOT), where red-detuned laser light causes a momentum transfer opposing the momentum of the atoms. Next the light is turned off and the atoms are trapped in a Magnetic Trap (MT) where the magnetic field causes a restoring force that traps the atoms. Using evaporative cooling, where the particles with the highest energy are removed using an RF field, the cloud is cooled even more. During the phase transition to BEC, the cooling process is sufficiently slow to minimize the probability of defects. If a cold cloud without a BEC is needed, the cooling step of

evaporative cooling is shorter, so more particles will be in the cloud. A more detailed description is in [2, Sec 2].

By the use of the MT, the atoms in the final cloud are all $F = 1$, $M_F = -1$ atoms. The specifications of the MOT don't really matter as long as enough particles at a certain temperature could be loaded to the MT. The MT is a harmonic trap within the boundaries of the experiment, and has a different strength in different directions. By the geometry of the magnetic coils a cylindrical symmetry is created in the trap. The MT can therefore be characterized by a radial and an axial trap frequency. The trap frequencies are measured by inducing a oscillation the cloud and determining the period of the oscillation of the center of mass of the cloud.

2.2 Imaging with PCI

After cooling our cloud (with or without a BEC) to the desired initial equilibrium, we start to take pictures of the cloud. A system in equilibrium has a unique density distribution for a certain trap, number of particles and the temperature. We analyze the pictures to get the chemical potential and temperature. Using Phase Contrast Imaging (PCI), there is very little interaction between the atoms and the light, causing only tiny changes in temperature and number of particles. We will take many pictures of the same cloud, that we analyze to determine the temperature and the number of particles, so we can determine some dynamics.

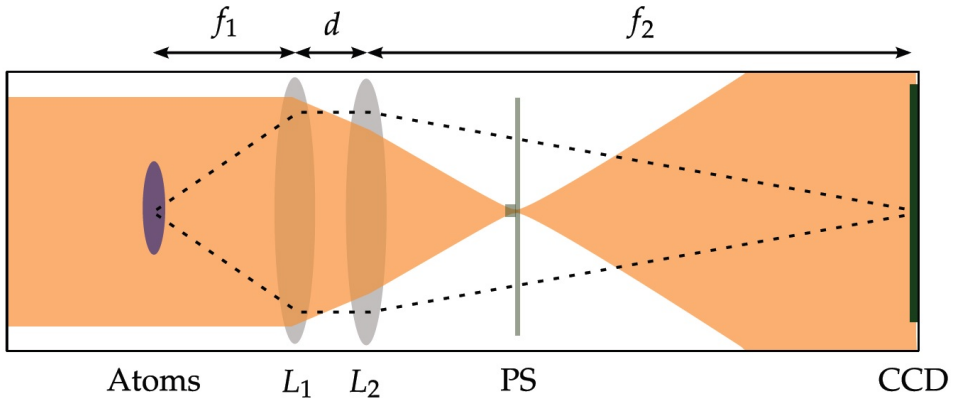

Figure 4: Schematic setup of the experimental of Phase Contrast Imaging (PCI), containing two lenses, a phase spot and a camera. The lightbeam is the yellow part. The dotted line produces a construction of the image of the atoms. (from R. Meppelink [2])

PCI is a technique which uses the phase shift of the light to determine the density profile. In Figure 4 a schematic setup is showed. A collimated beam passes through the atoms. Next the light passes through two lenses and a phase spot before the light hits

the camera. A phase spot is a transparent disk with a small cylindrical shaped hole in it. The hole has a diameter of 50μm and is $5/3\lambda$ deep where $\lambda = 589$nm the wavelength of the light. Some of the light passes through the atoms while an other part of the light goes around the atoms and through a phase spot, both hitting the camera where they interfere. So the intensity of the light on the camera depends on the angle θ introduced by the background and the phase angle ϕ_{atoms} by the atoms and the intensity with a phase spot without the atoms I_0. This intensity is derived in [2, Sec 3], with the following result of the transmission T

$$T = \frac{I}{I_0} = 3 - 2\cos(\theta) + 2\cos(\theta - \phi_{\text{atoms}}) - 2\cos(\phi_{\text{atoms}}) \tag{1}$$

During alignment, we first remove the second lens and get the phase spot shifted out of the beam. We place the second lens such that the background light focuses on the camera. The first lens is placed back, while the phase spot still remains shifted out of the beam. We align the first lens by making images of the cloud without a phase spot, where we aim to see 'nothing'. If the two lenses are aligned correctly and without an in-the-beam phase spot, we won't see the atoms, since we find a constant intensity independent of the phases caused by atoms, see Equation 1. If the two lenses aren't aligned correctly, defocussing occurs and there is some contrast due to the atoms, see [8]. Lastly we place the phase spot back in the beam, where the light is sufficiently focused at the phase spot to fit in the hole of the phase spot. We find a circular interference pattern if the phase spot is aligned correctly, aiding us in the alignment.

Three images are taken, one with laser light with the atoms with intensity I_{atoms}, one with laser light without the atoms with intensity I_0 and one without any laser light nor atoms to find the intensity of the background I_{bg}. The transmission T is given by:

$$T = \frac{I_{\text{atoms}} - I_{\text{bg}}}{I_0 - I_{\text{bg}}} \tag{2}$$

We use singular value decomposition (SVD) [6, Sec 3.4] to reduce noise in I_0.

For our measurements we need the intensity of the light in the cloud I_{cloud}. The intensity of the laser can be calculated from the number of counts per pixel on the camera, the count is average pixel value. The image of the cloud is enlarged by a factor 3 by the lenses, so the intensity of the light would be reduced by a factor $3^2 = 9$ before it hits the camera without any loss of light.

$$I_{\text{cloud}} = 9\frac{I_{\text{cam}}}{\eta} = 9\frac{1}{\eta q_e s}\frac{\mathcal{N}_i E_{\text{photon}}}{O t_{\text{exp}}} \tag{3}$$

The intensity of the laser light in the camera is $I_{\text{cam}} = I_0 - I_{\text{bg}}$. Further $\mathcal{N}_i = \mathcal{N}_{i,0} - \mathcal{N}_{i,\text{bg}}$ is the number counts per pixel of the i^{th} frame. The exposure time is t_{exp}. The energy of a photon is $E_{\text{photon}} = \hbar\omega = 3.37 \cdot 10^{-19}$J, the area of a pixel is $O = (8\mu\text{m})^2$. The probability for a photon which passes through a pixel to actually be detected by a pixel is $\frac{1}{q_e s}$ with q_e the quantum efficiency and s the sensitivity. Those depend on the mode of the camera called the Pre-Amplifier-Gain. If the Pre-Amplifier-Gain is 3.8, $q_e = 0.21$ and $s = 4.2$ (used in the experiment). If the Pre-Amplifier-Gain is 1, $q_e = 0.21$ and

$s = 1.63$. The efficiency coefficient η is the reduction of the light due to losses of light in mirrors and lenses. For all the measurements, including those of [1], until the beginning May 2014, $\eta = 0.19(2)$. This efficiently was low because some mirrors weren't placed as they were designed to. After moving the mirrors we find $\eta = 0.80(10)$.

2.3 The experiment and the analysis

Thus my experiment has several steps. First a cloud of atoms is prepared into the desired initial equilibrium, characterized by the trap frequencies, particle number and temperature. After this 100 images are taken using PCI rapidly ($\tilde{1}$0ms between two images) of the cloud. During those 100 photographs, the only dynamics are caused by the illumination of the laser and background effects. After we turn off our trap, the atoms are lost and we take twice another 100 images to determine I_0 and I_{bg}. Then a new cloud is created with similar initial conditions. We now take two pictures of new cloud, with 99 times more time between shots, to measure the background effects (in the assumptions that those are independent of the conditions of the cloud). We take multiple series of those images where we varied our initial conditions and the intensity of the light used.

In our analysis, we first determine the position of the center of mass by fitting our model (Popov) to the first few shots. Next, we fix the center of mass and fit our model to get the temperature, chemical potential, energy of the cloud and particle number for all frames. We determine the average change in temperature and particle number and subtract the background effects.

3 Theoretical predictions of the dynamics of an illuminated cloud

In this section a prediction is constructed for the dynamics of the cloud when illuminated. A expectation is made for the number of particles and the energy of the system per particle. The dynamics are caused by the photons.

In Section 3.1 the scattering rate is determined. The probability for the atom to get scattered by a photon to a different ground state is calculated in Section 3.2. The effect of a scattering event where an atoms falls back to a certain ground state is described in Section 3.3. In Section 3.4 a prediction for the dynamics of the particle number is generated, in Section 3.5 the energy of the system is described, and a prediction for the dynamics of the energy is generated. An enhancement in the scattering rate isn't included until Section 4.

3.1 The scattering rate

Sodium has different ground states and different excited states. The 8 ground states and 9 excited states are shown in Figure 5. A photon can be absorbed by an atom, called scattered. The atom will get excited before it almost instantly ($\gamma^{-1} = \tau \sim 16$ns) falls back to a (possibly different) ground state. The scattering rate is the number of scattering events per unit of time per atom and will be calculated in this section.

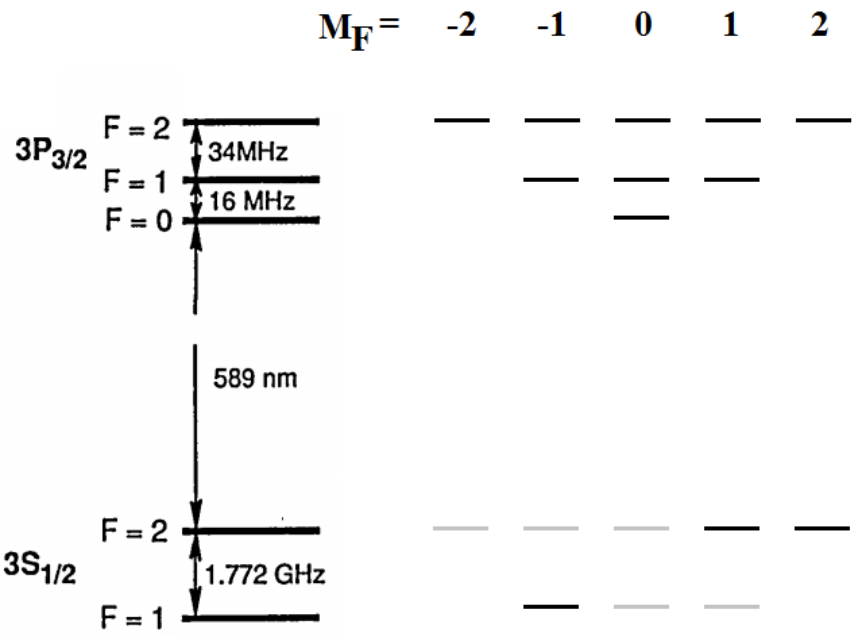

Figure 5: The 8 ground states and 9 excited states are shown. We start with all the atoms in the ground states $F = 1$, $M_F = -1$. The ground states $F = 1$, $M_F = -1$ and $F = 2$, $M_F = 1$ and $F = 2$, $M_F = 2$ are magnetically trapped, atoms in the other ground states (gray colored) won't feel the trap and will be lost. However only the ground state $F = 1$, $M_F = -1$ is also visible on PCI. The excited $F' = 3$ state is forbidden and therefore not drawn.

The scattering rate where light is scattered by atoms in the $F = 1$, $M_F = -1$ ground state that get excited to a $F' = e$ excited state is given by

$$\Gamma^e_{\text{sc}} = -\frac{I_{\text{cloud}}}{\hbar\epsilon_0 c}\text{Im}\left(\alpha^e(\beta)\right) \tag{4}$$

Here I_{cloud} denotes the intensity of the laser at the cloud, given in Equation 3, $\hbar$ the reduced Planks constant, ϵ_0 the vacuum permittivity and c the speed of light. The polarizability of the atoms is denoted with $\alpha^e(\beta)$ and depends on the transition to the

excited $F = e$ state. The polarizability is the ability for an atom to be polarized, causing the atom to produce a dipole moment. This dipole moment interacts with the electric field of the light. The polarizability of the atoms is given by

$$\alpha^e(\beta) = \frac{3i\epsilon_0\lambda^3}{4\pi^2}\frac{D_{F_e}(\beta)}{1 - 2i\delta_e/\gamma} \tag{5}$$

Here λ is the wavelength of the light, $\gamma = \tau^{-1}$ is the natural line width which is one over the lifetime τ of the excited stated and β is the angle between the polarization of the light and the quantization axis. For π-polarized light, we have $\beta = 0$, for linear combinations of σ^+ and σ^- we find $\beta = \pi/2$. The most important case is linear polarized light where the intensity of σ_+ equals the intensity of σ_- light. We have δ_e the detuning for the transition from the $F = 1$ to the excited $F' = e$ state

$$(\delta_0 \quad \delta_1 \quad \delta_2) = (\delta + 15.8\text{MHz} \quad \delta \quad \delta - 34.3\text{MHz}) \tag{6}$$

where we kept $\delta = 4 \times -86.5$ MHz (and occasionally $\delta = 2 \times -86.5$) and D_{F_e} the transition strengths of the transition from the $F = 1$ to the excited $F' = e$ state, given by

$$D_0(\beta) = \frac{4}{24}\sin^2\beta \qquad \xrightarrow{\beta=\pi/2} D_0 = \frac{4}{24} \tag{7}$$

$$D_1(\beta) = \frac{5}{24}(1 + \cos^2\beta) \qquad \xrightarrow{\beta=\pi/2} D_1 = \frac{5}{24} \tag{8}$$

$$D_2(\beta) = \frac{1}{24}(6 + \sin^2\beta) \qquad \xrightarrow{\beta=\pi/2} D_2 = \frac{7}{24} \tag{9}$$

3.2 Probability to get to an different ground state

When a photon scatters on an atom, the atom gets excited and fall back to a ground state. The atoms are illuminated with linear polarized light where the intensity of σ_+ and σ_- is equal. Here the probability of an atom, to get excited and fall back to the ground state with $F = 1$ or $F = 2$, is calculated for a given scattering rate. All the particles start in the ground state $F = 1$ and $M_F = -1$.

First the probability to get to a certain exited state is determined. Those probabilities are denoted with a vector. We ignore the $F = 3$ state since this isn't reached, so only the excited states 1 times the $F = 0$ state plus 3 times the $F = 1$ state plus 5 times the $F = 2$ state are considered. So the probabilities to get to the 9 relevant exited states can be denoted with a vector in the $\mathbb{R}^1 \oplus \mathbb{R}^3 \oplus \mathbb{R}^5$ space. If we consider just π-polarized light, we have the angle between the polarization of the light and the quantization axis $\beta = 0$. We only get to the $F = 1$, $M_F = -1$ and the $F = 2$, $M_F = -1$ state, those probabilities are given by

$$\phi_{E,\pi} = t_{\text{exp}}(0 \quad \Gamma^1_{\text{sc}} \quad 0 \quad 0 \quad 0 \quad \Gamma^2_{\text{sc}} \quad 0 \quad 0 \quad 0)^\top \tag{10}$$

with t_{exp} the time of illumination per frame. Here Γ^e_{sc} is the scattering rate given in Equation 4. If we consider linear polarized with the intensity of the σ_+ equal to the intensity of the σ_- light, we get $\beta = \pi/2$ and

$$\phi_{E,\sigma} = t_{\text{exp}}(\Gamma^0_{\text{sc}} \quad 0 \quad \Gamma^1_{\text{sc}} \quad 0 \quad \tfrac{6}{7}\Gamma^2_{\text{sc}} \quad 0 \quad \tfrac{1}{7}\Gamma^2_{\text{sc}} \quad 0 \quad 0)^\top \tag{11}$$

It turns out that the difference between linear σ-polarized light and linear π-polarized light are minimal ($\sim$2%). In the rest of the calculation we will only consider linear σ-polarized light, also used in our experiment, and we use Equation 11. Now the probability to fall back from an excited state to the different ground state is calculated. There are 8 relevant ground states, 3 from the $F = 1$ and 5 from the $F = 2$ ground state. So a vector of probabilities to get to the different ground states in the $\mathbb{R}^3 \oplus \mathbb{R}^5$ space is used.

Without restrictions, the atoms could fall back from 9 excited states to 8 ground states, though by certain restrictions some probabilities are zero. This is denoted with a 9×8 matrix. We separate the cases where π, σ_+ and σ_--polarize light is emitted. Those probabilities are the Clebsch Gordan coefficient and denoted with the matrices: $\mathcal{S}_\pi$, $\mathcal{S}_{\sigma^+}$, $\mathcal{S}_{\sigma^-}$, where the total probability to fall back to a state is given by $\mathcal{S} = \mathcal{S}_\pi + \mathcal{S}_{\sigma^+} + \mathcal{S}_{\sigma^-}$. The values for $\mathcal{S}$ are given in Equation 13.

The probability to get excited and fall back to a certain ground state is just the product of the probability to get excited and the probability to fall back, summed over the different ways to get to the new ground state. In linear algebra this could be written as a matrix multiplication. The probability to get excited and fall back to the ground states is denoted with ϕ_G

$$\phi_G = (\mathcal{S}_{\sigma^-} + \mathcal{S}_{\sigma^+} + \mathcal{S}_\pi) \cdot \phi_{E,\sigma} \tag{12}$$

So by calculating this all, a vector for the probabilities to get excited and fall back to a ground state ϕ_G is found

$$S_{\sigma^-} = \tfrac{1}{60}\begin{pmatrix} 0 & 0 & 20 & 0 & 0 & 0 & 0 & 0 \\ 0 & 25 & 0 & 0 & 0 & 1 & 0 & 0 \\ 0 & 0 & 25 & 0 & 0 & 0 & 3 & 0 \\ 0 & 0 & 0 & 0 & 0 & 0 & 0 & 6 \\ 30 & 0 & 0 & 0 & 10 & 0 & 0 & 0 \\ 0 & 15 & 0 & 0 & 0 & 15 & 0 & 0 \\ 0 & 0 & 5 & 0 & 0 & 0 & 15 & 0 \\ 0 & 0 & 0 & 0 & 0 & 0 & 0 & 10 \\ 0 & 0 & 0 & 0 & 0 & 0 & 0 & 0 \end{pmatrix}^\top \qquad S_\pi = \tfrac{1}{60}\begin{pmatrix} 0 & 25 & 0 & 0 & 0 & 15 & 0 & 0 & 0 \\ 20 & 0 & 0 & 0 & 0 & 0 & 20 & 0 & 0 \\ 0 & 0 & 0 & 25 & 0 & 0 & 0 & 15 & 0 \\ 0 & 0 & 0 & 0 & 20 & 0 & 0 & 0 & 0 \\ 0 & 3 & 0 & 0 & 0 & 5 & 0 & 0 & 0 \\ 0 & 0 & 4 & 0 & 0 & 0 & 0 & 0 & 0 \\ 0 & 0 & 0 & 3 & 0 & 0 & 0 & 5 & 0 \\ 0 & 0 & 0 & 0 & 0 & 0 & 0 & 0 & 20 \end{pmatrix}$$

$$S_{\sigma^+} = \tfrac{1}{60}\begin{pmatrix} 20 & 0 & 0 & 0 & 0 & 0 & 0 & 0 \\ 0 & 0 & 0 & 6 & 0 & 0 & 0 & 0 \\ 25 & 0 & 0 & 0 & 3 & 0 & 0 & 0 \\ 0 & 25 & 0 & 0 & 0 & 1 & 0 & 0 \\ 0 & 0 & 0 & 0 & 0 & 0 & 0 & 0 \\ 0 & 0 & 0 & 10 & 0 & 0 & 0 & 0 \\ 5 & 0 & 0 & 0 & 15 & 0 & 0 & 0 \\ 0 & 15 & 0 & 0 & 0 & 15 & 0 & 0 \\ 0 & 0 & 30 & 0 & 0 & 0 & 10 & 0 \end{pmatrix}^\top \qquad \phi_G = t_{exp}\begin{pmatrix} \frac{1}{3}\Gamma^0_{sc} + \frac{5}{12}\Gamma^1_{sc} + \frac{37}{84}\Gamma^2_{sc} \\ \frac{1}{3}\Gamma^0_{sc} + \frac{1}{21}\Gamma^2_{sc} \\ \frac{1}{3}\Gamma^0_{sc} + \frac{5}{12}\Gamma^1_{sc} + \frac{1}{84}\Gamma^2_{sc} \\ \frac{2}{7}\Gamma^2_{sc} \\ \frac{1}{20}\Gamma^1_{sc} + \frac{5}{28}\Gamma^2_{sc} \\ \frac{1}{15}\Gamma^1_{sc} \\ \frac{1}{20}\Gamma^1_{sc} + \frac{1}{28}\Gamma^2_{sc} \\ 0 \end{pmatrix} \tag{13}$$

A quick example of calculating with the probability. Consider the case for an atom in the ground state $F = 1$, $M_F = -1$ to get excited to the $F' = 1$, $M_F = 0$ and fall back to the ground state $F = 1$, $M_F = 1$. The probability to get excited to the $F' = 1$,

$M_F = 0$ state is the 3^{th} element of $\phi_{E,\sigma}$ is $t_{exp}\Gamma^1_{sc}$. The probability to fall back to the $F = 1$, $M_F = 1$ ground state is the element (3,3) of $\mathcal{S}$ is $\mathcal{S}_{3,3} = \frac{25}{60}$. The product is $t_{exp}\frac{25}{60}\Gamma^1_{sc}$, which contributes to the total probability to get to the $F = 1$, $M_F = 1$ state $\phi_{G,3} = \frac{1}{3}\Gamma^0_{sc} + \frac{5}{12}\Gamma^1_{sc} + \frac{1}{84}\Gamma^2_{sc}$, the 3^{th} element of ϕ_G. Their are different routes to get to this ground state $F = 1$, $M_F = 1$, and those probabilities should be summed over.

3.3 The effect of scattering on the system

If a photon is scattered on a atom, the atom gets a momentum transfer from the photon, in the direction of the light from the absorption and in a random direction from the emission of the photon. A photon has a momentum of $p = \frac{\hbar\omega}{c}$. We have to use the average energy transfer $(\frac{p^2_{\text{transfer}}}{2m})_{\text{avg}}$, with p_{transfer} the total momentum transfered by two photons. With

$$p^2_{\text{transfer}} = \left(\frac{\hbar\omega}{c}\right)^2 \frac{1}{4\pi}\int_0^{\pi} \mathrm{d}\theta \int_0^{2\pi} \mathrm{d}\phi \sin\theta \left|\left|\begin{matrix}\sin\theta\cos\phi \\ \sin\theta\sin\phi \\ 1+\cos\theta\end{matrix}\right|\right|^2 = 2\left(\frac{\hbar\omega}{c}\right)^2 \tag{14}$$

So the energy increase is $\frac{p^2_{\text{transfer}}}{2m} = \frac{\hbar^2\omega^2}{mc^2}$. The energy increase is independent of the initial moment p_0 since the new energy minus the old energy is just the energy of the transfered momentum.

$$\begin{matrix}\frac{1}{4\pi}\int_0^{\pi}\mathrm{d}\theta\int_0^{2\pi}\mathrm{d}\phi\sin\theta\times \\ \frac{(p_{\text{transfer}}+p_0\cos\theta)^2+(p_0\sin\theta\sin\phi)^2+(p_0\sin\theta\cos\phi)^2-p_0^2}{2m}\end{matrix} = \frac{p^2_{\text{transfer}}}{2m} \tag{15}$$

We consider a cloud in the hydrodynamic limit, so all scattered particle redistribute their energy and give an energy increase per particle.

$$E_{pp} = (1,1,1,1,1,1,1,1)\cdot\phi_G\cdot\frac{\hbar^2\omega^2}{mc^2} = t_{\text{exp}}\left(\Gamma^0_{sc}+\Gamma^1_{sc}+\Gamma^2_{sc}\right)\frac{\hbar^2\omega^2}{mc^2} \tag{16}$$

The vector ϕ_G of probabilities to get to a different ground state is used, see Equation 13. For a small cloud this is not always the case. Let us consider the dilute limit. The fraction of particles lost remains the same, though the energy increase per scatter event decreases. This decrease is because particles no longer trapped don't redistribute their gained energy. Only particles still trapped will redistribute their energy.

$$E_{pp} = \frac{\hbar^2\omega^2}{mc^2}(1,0,0,0,0,0,1,1)\cdot\phi_G = t_{\text{exp}}\left(\frac{1}{3}\Gamma^0_{sc}+\frac{5}{12}\Gamma^1_{sc}+\frac{37}{84}\Gamma^2_{sc}\right)\frac{\hbar^2\omega^2}{mc^2} \tag{17}$$

The fraction of the particles lost, is given by the sum of the product of the probabilities to get to a certain state times the probabilities of a certain state to be no longer trapped (this is either 0 or 1). The fraction of atoms no longer trapped is

$$g = (0,1,1,1,1,1,0,0)\cdot\phi_G = t_{\text{exp}}\left(\frac{2}{3}\Gamma^0_{sc}+\frac{7}{12}\Gamma^1_{sc}+\frac{47}{84}\Gamma^2_{sc}\right) \tag{18}$$

3.4 The number of particles

Here an expression for the dynamics in the number of particles is calculated. If N_i denotes the total number of particles, and g_i the fraction of the particles lost after the N_i^{th} frame, then the expression for N_i is:

$$N_{i+1} = N_i(1 - g_i) \tag{19}$$

If the enhancement is constant, the fraction of atoms scattered is constant. For a cloud without BEC this is the case. For a cloud with a BEC, when there is a minimal change of the system within a series of frames, we can approximate this as well. If $g_i = g \ll 1$ is constant an expression is

$$N_i = N_0(1 - g)^i \approx N_0 \exp(-g \cdot i) \tag{20}$$

The fraction of the particles lost g is the sum of all probabilities to a scattering event where the particle is lost, calculated in Equation 18.

3.5 The energy

Here an expression for the energy of the system is calculated. The energy per particle for particles in a harmonic trap is calculated with [5, Sec 2.4]

$$E = 3Nk_BT\frac{\zeta(4)}{\zeta(3)}\left(\frac{T}{T_c}\right)^3 + \frac{5}{7}2\pi\hbar\mu \qquad T \leq T_c \tag{21}$$

$$E = 3Nk_BT\left[1 + \frac{\zeta(3)}{2^4}\left(\frac{T_c}{T}\right)^3\right] \qquad T > T_c \tag{22}$$

Here $2\pi\mu\hbar$ is the chemical potential which has negligible effect. Here k_B is the Boltzmann constant, T the temperature, $T_c = \frac{\hbar\bar{\omega}N^{1/3}}{(\zeta(3))^{1/3}}$ the critical temperature as a function of the number of particles, $\hbar$ the reduced Planck constant and $\bar{\omega} = (\omega_x\omega_y\omega_z)^{1/3}$ the average of the trap frequencies. The Riemann Zeta function is denoted with ζ. For $T \gg T_c$ we find the classical expression $E \approx 3Nk_BT \propto N$. However, for $T \leq T_c$ we find that the energy is independent of the total number of particles, since the thermal cloud is saturated and the condensed particles have a negligible amount of energy.

We include two effects caused by the scattering, the momentum transfer and the loss of particles. The effect on the energy of the system by the momentum transfer for one particle was described in Section 3.3. Now the effect on the energy of the system of the loss of particles is described.

If only atoms are lost (without an explicit change in energy per particle), a decrease in number of atoms is noticed. For a given temperature, if a fraction of particles is removed, we expect also to remove a fraction of the total energy. So

$$\Delta E_{\text{expect}} = \Delta N\frac{E}{N} = \frac{\Delta N}{N}E \tag{23}$$

We consider two cases, $E \propto N$ for a cloud without a BEC and $E \not\propto N$ for a cloud with a BEC where E is independent of the number of particles. We calculate directly $\Delta E \equiv E(N + \Delta N) - E(N)$.

$$\Delta E_{T>T_c} = E\frac{N + \Delta N - N}{N} = E\frac{\Delta N}{N} \qquad \text{if } E \propto N \tag{24}$$

$$\Delta E_{T<T_c} = E - E = 0 \qquad \text{if } E \not\propto N \tag{25}$$

So for $T > T_c$ and $E \propto N$ we have removed also a fraction of the total energy as expected. Equation 23 and Equation 24 agree. No explicit energy decrease has to be introduced.

However for $T < T_c$ the energy is independent of the number of particles $E \not\propto N$. Now we do not find a direct decrease in energy. So by removing some particles we remove some energy which is not found directly. Equation 23 and Equation 25 do not agree. We have to add an additional energy per particle decreasing term $\Delta E = \frac{\Delta N}{N} E$ to make the equations agree.

If a thermal particle is lost in a cloud with a BEC, we expect a BEC particle to get thermal to keep the thermal cloud saturated. This effect is a cooling effect, and gives an intuitive explanation of the previous explicit energy decreasing term.

Dynamic energy expression for $T > T_c$

Here an expression for the dynamics of the energy of the system is calculated for a cloud without a BEC. If $\mathcal{E}_i = E_i/N_i$ denotes the average energy per particle in the i$^{\text{th}}$ frame, for $T > T_c$, $\mathcal{E}_{i+1}$ is given by

$$\mathcal{E}_{i+1} = \mathcal{E}_i + E_{pp,i} \tag{26}$$

If the enhancement is constant, the fraction of atoms scattered is constant. For a cloud without BEC this is the case. For a cloud with a BEC, when there is a minimal change of the system within a series of frames, we can approximate this as well. Then the expression becomes

$$\mathcal{E}_i = \mathcal{E}_0 + iE_{pp} \tag{27}$$

we can approximate the energy with an expression for the temperature.

$$T_i \approx T_0 + i\frac{E_{pp}}{3k_B} \tag{28}$$

with E_{pp} energy added per frame. The temperature change is the energy change over the heat capacity per particle $C_V^* \approx 3k_B$. This is the probability for an atom to scatter times the average energy added, calculated in Equation 16.

Dynamic energy expression for $T < T_c$

Here an expression for the dynamics of the energy of the system is calculated for a cloud with a BEC. For $T < T_c$, we will add an explicit cooling term in our equation for the energy per particle. This is necessary since during the remove particles we also lose energy we haven't included yet. Our equation for the average energy per particle becomes

$$\mathcal{E}_{i+1} = \mathcal{E}_i + E_{pp,i} - g_i \mathcal{E}_i \tag{29}$$

If $E_{pp,i} = E_{pp}$ and $g_i = g$ are constant (this can be approximated when the system has minimal changes and a constant enhancement in the scattering rate), this can be written as a differential equation:

$$\dot{\mathcal{E}} = E_{pp} - g\mathcal{E} \tag{30}$$

We solve this and find

$$\mathcal{E}_i = \frac{E_{pp}}{g} + \frac{\mathcal{E}_{i_0} - \frac{E_{pp}}{g}}{\exp(-gi_0)} \exp(-gi) \tag{31}$$

This function will have an asymptotic value at $\mathcal{E} = \frac{E_{pp}}{g}$.

4 The enhanced scattering rate

In the calculation for the polarizability an extra factor $\frac{1}{1+A}$ is introduced due to neighboring atoms. Equation 5 will get this extra factor. This factor will also enhance the scattering rate as given in Equation 4.In this section an expression for A is calculated, see also [3, Eq 24] (denoted by C) and [4, Sec 3]. The factor $\frac{1}{1+A}$ introduced in the polarizability of the atom α at the probe frequency, gives an correction for the:
1-Standard Lorentz-Lorenz local field correction.
2-Two-body correlation function.
*An effect of dipole-dipole interaction is not included since in would be small since it depends quadratically on the polarizability $\alpha \ll 1$.

The equation for A is

$$A \equiv \underbrace{-\frac{1}{3}\alpha\rho_0}_{\text{Lorentz-Lorenz}} \underbrace{-\alpha\rho_0 \int \mathrm{d}^3 r \widetilde{g}_{xx}(\vec{r}) e^{-ik_m z} \phi(r)}_{\text{Two-body correlation function}} \tag{32}$$

where α is the polarizability and ρ_0 the local density the pair correlation function is denoted with $\phi(r)$, which is called also the two body correlation function, given in Section 4.1. In Section 4.2 an expression for $\widetilde{g}_{xx}(\vec{r})$ is given in and simplified. Since the local density approximation is used, we have to average over the cloud in Section 4.3. In Section 4.4 we will verify the converging of the integral expression of A. Finally we verify the local density approximation in Section 4.5, by showing the integral converges within the dimensions of the condensate.

4.1 The pair correlation function $\phi(u)$ and density function $\rho(r)$

The pair correlation function is shown in Figure 6a for some values, will be calculated here. For $T > T_c$ and $T \leq T_c$ with T_c the critical temperature there are two different formulas for the pair correlation function.

$$\phi(u) = \begin{cases} \left[\frac{g_{3/2}\left(\alpha_s, \pi\frac{u^2}{\lambda_{DB}^2}\right)}{\rho_0\lambda_{DB}^3}\right]^2 & T > T_c \\ \left[1 - \frac{g_{3/2}(0)}{\rho_0\lambda_{DB}^3} + \frac{g_{3/2}\left(\pi\frac{u^2}{\lambda_{DB}^2}\right)}{\rho_0\lambda_{DB}^3}\right]^2 - \left[1 - \frac{g_{3/2}(0)}{\rho_0\lambda_{DB}^3}\right]^2 & T \leq T_c \end{cases} \tag{33}$$

Also $g_{3/2}$ is defined as

$$g_{3/2}(\alpha_s, x) = \sum_{n=1}^{\infty} n^{-3/2} \exp(n\alpha_s - x/n) \tag{34}$$

where $0 \geq \alpha_s = \frac{1}{k_B T}\min(\mu_0, 0) = \log\left[g_{3/2}^{-1}(\rho_0\Lambda_{DB}^3)\right]$ and $\alpha_s = 0$ appears when there is a condensate. Here $\Lambda_{DB} = \sqrt{\frac{2\pi\hbar^2}{mk_B T}}$ is the thermal De Broglie wavelength and $\rho_0 = \rho(\vec{r}_0)$ is the local density, $\mu_0 = \mu - V(\vec{r}_0)$ is the local chemical potential. Those are kept constant during the local density approximation and calculating the relative enhancement of the scattering rate at a certain point, though variated when averaging the relative enhancement of the scattering rate over space. We define $g_{3/2}(x) = g_{3/2}(0, x)$ and note $g_{3/2}(0) \approx 2.612$.

Now techniques will be used to determine $g_{3/2}$ more efficient numerically. Instead of summing infinite terms, sum a finite number of terms and integrate over the rest, dramatically reducing the number of terms before convergence is reached. First have a look at $T \leq T_c$, where we have $g_{3/2}\left(\pi\frac{u^2}{\lambda_{DB}^2}\right)$.

$$\begin{aligned} g_{3/2}\left(\pi\frac{u^2}{\lambda_{DB}^2}\right) &= \sum_{n=1}^{\infty} \frac{\exp\frac{-\pi u^2}{n\lambda_{DB}^2}}{n^{3/2}} \\ &\approx \sum_{n=1}^{N} \frac{\exp\frac{-\pi u^2}{n\lambda_{DB}^2}}{n^{3/2}} + \int_N^{\infty} \mathrm{d}n \frac{\exp\frac{-\pi u^2}{n\lambda_{DB}^2}}{n^{3/2}} \\ &= \sum_{n=1}^{N} \frac{\exp\frac{-\pi u^2}{n\lambda_{DB}^2}}{n^{3/2}} + \frac{\lambda_{DB}\mathrm{erf}\left(\frac{\sqrt{\pi}u}{\sqrt{N}\lambda_{DB}}\right)}{u} \end{aligned} \tag{35}$$

This can be done also for $T > T_c$, where $g_{3/2}\left(\alpha_s, \pi\frac{u^2}{\lambda_{DB}^2}\right)$.

$$\begin{aligned} g_{3/2}\left(\alpha_s, \pi\frac{u^2}{\lambda_{DB}^2}\right) &= \sum_{n=1}^{\infty} \frac{\exp\left(\frac{-\pi u^2}{n\lambda_{DB}^2} + \alpha_s n\right)}{n^{3/2}} \\ &\approx \sum_{n=1}^{N} \frac{\exp\left(\frac{-\pi u^2}{n\lambda_{DB}^2} + \alpha_s n\right)}{n^{3/2}} + \int_N^{\infty} \mathrm{d}n \frac{\exp\left(\frac{-\pi u^2}{n\lambda_{DB}^2} + \alpha_s n\right)}{n^{3/2}} \\ &= \left(\sum_{n=1}^{N} \frac{\exp\left(\frac{-\pi u^2}{n\lambda_{DB}^2} + \alpha_s n\right)}{n^{3/2}}\right) + \frac{\lambda_{DB}}{2u}\Bigg[\\ &\quad \exp\left(-\frac{2\sqrt{\pi}u\sqrt{-\alpha_s}}{\lambda_{DB}}\right) \mathrm{erfc}\left(\sqrt{-N\alpha_s} + \frac{\sqrt{\pi}u}{\sqrt{N}\lambda_{DB}}\right) - \\ &\quad \exp\left(\frac{2\sqrt{\pi}u\sqrt{-\alpha_s}}{\lambda_{DB}}\right) \mathrm{erfc}\left(\sqrt{-N\alpha_s} - \frac{\sqrt{\pi}u}{\sqrt{N}\lambda_{DB}}\right)\Bigg] \end{aligned} \tag{36}$$

With erfc the complementary error function. Picking the value for N large enough for which the result is converged, is essential. However a small N will reduce the calculation time. It turns out that a value of $N = 10$ seems to be sufficiently large.

4.2 Towards calculating A

Again the definition of A as in Equation 32

$$A \equiv -\frac{1}{3}\alpha\rho_0 - \alpha\rho_0 \int \mathrm{d}^3 r \widetilde{g}_{xx}(\vec{r}) e^{-ik_m z} \phi(r) \tag{37}$$

Here $\phi(\vec{r})$ was the pair correlation function given in Section 4.1 and $g_{\alpha\beta} = \widetilde{g}_{\alpha\beta} - \frac{1}{3}\delta_{\alpha\beta}\delta(\vec{r})$ where $\widetilde{g}_{\alpha\beta}$ and $\widetilde{g}_{xx}$ given by:

$$\widetilde{g}_{\alpha\beta} = \widetilde{g}_0 \left[\left(1 + \frac{3i}{k_c r} - \frac{3}{(k_c r)^2}\right)\frac{r_\alpha r_\beta}{r^2} - \left(1 + \frac{i}{k_c r} - \frac{1}{(k_c r)^2}\right)\delta_{\alpha\beta}\right] \tag{38}$$

$$\widetilde{g}_{xx} = \widetilde{g}_0 \left[\left(1 + \frac{3i}{k_c r} - \frac{3}{k_c^2 r^2}\right)(\cos\zeta \sin\theta)^2 - \left(1 + \frac{i}{k_c r} - \frac{1}{k_c^2 r^2}\right)\right] \tag{39}$$

Where $\widetilde{g}_0 = -\frac{k_c^3}{4\pi}\frac{e^{ik_c r}}{k_c r}$, $k_c = k\sqrt{1 + \alpha\rho_0}$ and $k_m = k\sqrt{1 + \frac{\alpha\rho_0}{1+A}}$. Here $\alpha = \sum_e \alpha^e$ is the total polarizability and $k = \frac{2\pi}{\lambda}$ is the wave number of the light in vacuum. In a medium the wavenumber is different, k_c and k_m can be seen as the wave number in the medium, the imaginary part of $k_c, k_m \in \mathbb{C}$ can be seen as scattering events. Even though $|A|, |\alpha\rho| \ll 1$, it turns out that these terms are necessary to make the integral converge, see Section 4.4.

Substitute spherical coordinates and Jacobian $r^2 \sin\theta$. Integrate over the angle of the integral of Equation 37. This is easy since the pair correlation function $\phi(r) = \phi(|r|)$ is

independent of the angle. For notation purposes the result is called $\frac{h(r)}{k}$

$$\frac{h(r)}{k} = \frac{1}{k}\int_0^{\pi} \mathrm{d}\theta \int_0^{2\pi} \mathrm{d}\zeta \;\; r^2 \sin\theta \; \widetilde{g}_{xx}(r,\theta,\zeta) e^{-ik_m r\cos\theta} \tag{40}$$

$$= \frac{k_c}{k}\frac{e^{ik_c r}(k_c r)^2}{(k_c r)^3 (k_m r)^3}\Big\{k_m r\cos(k_m r)\Big[-3 + k_c r(3i + k_c r)\Big] + \sin(k_m r)\Big[3 - k_c r(3i + k_c r) + k_m^2 r^2(-1 + ik_c r + k_c^2 r^2)\Big]\Big\} \tag{41}$$

One can find that $\lim_{r\to 0} h(r)$ exists and is zero, so the bottom part of the integral converges. To make sure that no numerical errors will occur, we use a Taylor approximation around zero, for small values of r.
Since k_c has an imaginary part, the term $e^{ik_c r}$ will give a damping factor to make the top part of the integral converge (Section 4.4 will give some calculations).

Now a formula (iterating since k_c depends on A) is found, which can be integrated numerical for Equation 32, where $u = kr$ is substituted. For typical values three iteration steps are sufficient (starting with $A_0 = -\frac{1}{3}\alpha\rho$).

$$\frac{A}{\alpha\rho_0} = -\frac{1}{3} - \int_0^{\infty} h(r)\phi(k\,r)\mathrm{d}r = -\frac{1}{3} - \int_0^{\infty} \frac{h(\frac{u}{k})\phi(u)}{k}\mathrm{d}u \tag{42}$$

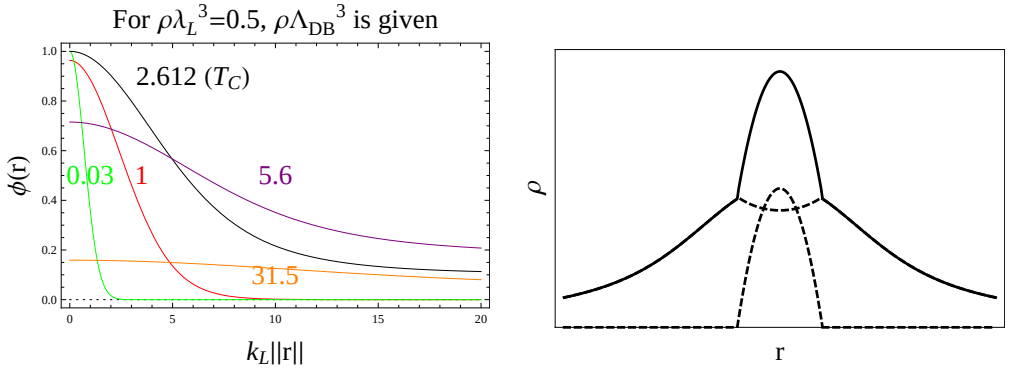

(a) (b)

Figure 6: In (a) the pair correlation function is shown, with λ_L the wavelength of the light and $\Lambda_D B$ the de Broglie wavelength. The numbers represent the value of $\rho\Lambda_{DB}^3$. For T_c their is $\rho\Lambda_{DB}^3 = g_{3/2}(0) \approx 2.612$. In (b) the density function is shown, where the dotted parts are the thermal and condensed part and the solid part is the total density.

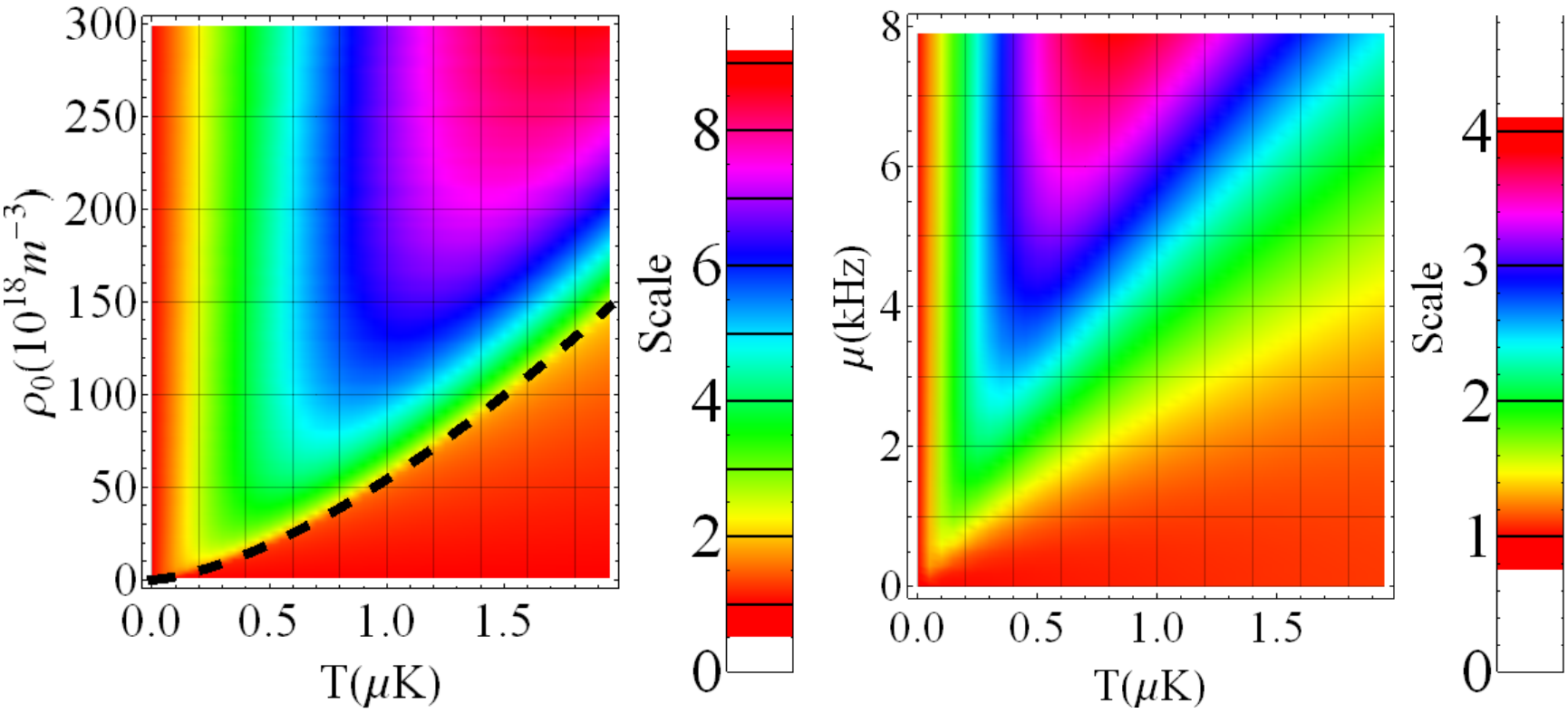

Figure 7: The relative enhanced scattering rate for sodium with a detuning of $\delta = -346$MHz is showed here. In (a) is this a function of the temperature T and density ρ_0 in a homogeneous system, where the dashed line denoted the critical temperature $T_c = \left(\frac{\rho}{\zeta(3/2)}\right)^{2/3} \frac{2\pi\hbar^2}{mk_B}$. In (b) the cloud with a density distribution due to a harmonic trap this relative enhanced scattering rate is averaged over the cloud, where the system is characterized by the temperature T and the chemical potential μ.

4.3 Averaging over the cloud

In the calculation A depends on the local density, so we use the local density approximation. We calculate A (and iterate) for a fixed density and take the average factor $\left\langle \frac{1}{1+A} \right\rangle$ over all particles. We denote the local density around particle with index n as $\rho(n) = \rho(\vec{r}(n))$. We simplify this by integrating over space.

$$\left\langle \frac{1}{1+A} \right\rangle = \frac{\sum_{n=1}^{N} \frac{1}{1+A(\rho(n))}}{N} = \frac{\int \frac{\mathrm{d}\vec{r}\rho(\vec{r})}{1+A(\rho(\vec{r}))}}{N} = \frac{\int_0^\infty \int_0^\infty \frac{\mathrm{d}r\ \mathrm{d}z\ 4\pi r\rho(r,z)}{1+A(\rho(r,z))}}{N} \tag{43}$$

In the easiest approximation where thermal and condensed atoms do not interact, the density function $\rho(\vec{r})$ consists out of two parts, the density of the thermal cloud is added with the density of the condensed atoms.

$$\rho(r) = g_{3/2}\left(\frac{|\mu - V(r)|}{k_B T}\right) + \frac{\max(0, \mu - V(r))}{u_0} \tag{44}$$

The density function is shown in Figure 6b This value of for the density is used in the local density approximation. When a fit is made to our images we use Popov approximation to determine the temperature and chemical potential.

Now we will calculate the relative enhancement of the scattering rate, which is the total enhanced scattering rate over the total non enhanced scattering rate. Since the imaginary and real part of $\frac{1}{1+A}$ part will mix up, it is necessary to include the $\frac{1}{1-2i\delta_e/\gamma}$ in the calculation. Constant terms will cancel.

$$\text{rel.enhan} = \frac{\sum_e \Gamma^e_{sc}}{\sum_e \Gamma^e_{sc,\ \text{non enh}}} = \frac{\mathrm{Im}\left(\sum_e \left\langle \frac{1}{1+A} \right\rangle \frac{1}{1-2i\delta_e/\gamma}\right)}{\mathrm{Im}\left(\sum_e \frac{1}{1-2i\delta_e/\gamma}\right)} \tag{45}$$

with $\Gamma^e_{sc,\ \text{non enh}}$ the non enhanced scattering rate. In Figure 7 the relative enhancement is plotted as a function of temperature T and the density ρ_0. We also average over the cloud and the relative enhancement as function of the temperature T and the chemical potential μ under typical experimental conditions (using sodium, detuning $\delta = -346$MHz).

4.4 Making the integral A converge

Here first, the pair correlation function in the limit $r \to \infty$ is calculated, this is necessary to determine whether the integral expression for A converges. First take $u \to \infty$ of the $g_{3/2}$ function, use Section 4.1. Note that the finite sum goes exponentially to zero, since the elements goes exponentially to zero.

It turns out for $T > T_c$ that the complementary error function multiplied by the exponent divided by r are going to zero even faster. So above the critical temperature the $g_{3/2}$ function is going to zero sufficiently fast to integrate over space. Since $\phi(u) \propto (g_{3/2})^2$,

the pair correlation function will also converge to zero sufficiently fast to integrate over space (exponentially or faster).

Below $T_c > T$ it turns out that the $g_{3/2}$ function goes as $1/u$ for $u \to \infty$. With some calculations we find that $\phi(u) = C_1 g_{3/2} + C_2 (g_{3/2})^2$ for $C_{1,2}$ independent of u. So $\phi(u)$ goes as $1/u$ below the critical temperature.

First it is shown that the integral will diverge if we make an incorrect (though intuitive acceptable, and also not always explicitly and clearly written down in the literature as [4, Section 3] and [3]) approximation. After this it is shown that the integral will converge without these approximations.

Notice $|A_0|, |\alpha\rho| \ll 1$ and $k_c = k\sqrt{1+\alpha\rho_0}$ and $k_m = k\sqrt{1+\frac{\alpha\rho_0}{1+A}}$. In the approximation $k_c = k_m = k$ we find:

$$\frac{h(u)}{k} = e^{iku}\left(\frac{ku(-3+3iku+(ku)^2}{(ku)^4}\cos(ku)+ \right. \\ \left. \frac{3-3iku-2(ku)^2+i(ku)^3+(ku)^4}{(ku)^4}\sin(ku)\right) \tag{46}$$

For $kr \gg 1$ we find $\frac{h(u)}{k} \to \sin(ku)(\cos(ku) + i\sin(ku))$, where the imaginary part oscillates around a non-zero number, $1/2$. The pair correlation function will give a $1/u$ term, which combined will go as $1/u$, this will make the integral diverge as $\log(u)$.

We have found that in the approximation $k_c \to k$ and $k_m \to k$, the integral A diverges. Without these approximation, we find that the $h(u)/k$ function will go exponentially to zero since the e^{ik_c} will have a negative real part in the exponent.

4.5 Validating the local density approximation

As was read in Section 4.4, we had some difficulty making the integral converge. The local density approximation assumes that the density is locally constant. This is the case if the integral would be converging fast enough (within the dimensions of the condensate), which is not trivial.

After calculating the relative enhancement of the scattering rate (Equation 45) depending on A (Equation 32), with the difference that A was calculated after integrating over a finite volume, showed that the relative enhancement of the scattering rate has got for typical values approximately 50% and 90% of it's value after just 0.001mm and 0.01mm. This could be explained since the scattering length only take the exponential damping into account, but it doesn't take the $1/r$ damping of the pair correlation function (see Section 4.4). Since $1/r$ will give a logarithm out of the integral, the factor would be strongly damped, since the effect of the volume of 0.1mm to 1mm will be as small as 0.0001mm to 0.001mm. So the experimental situation will have in good approximation, probably around 90%, the same effect as the calculated homogeneous situation. In Figure 8 polarizability with the relative enhancement of the scattering rate as a function of T is calculated for typical experimental conditions.

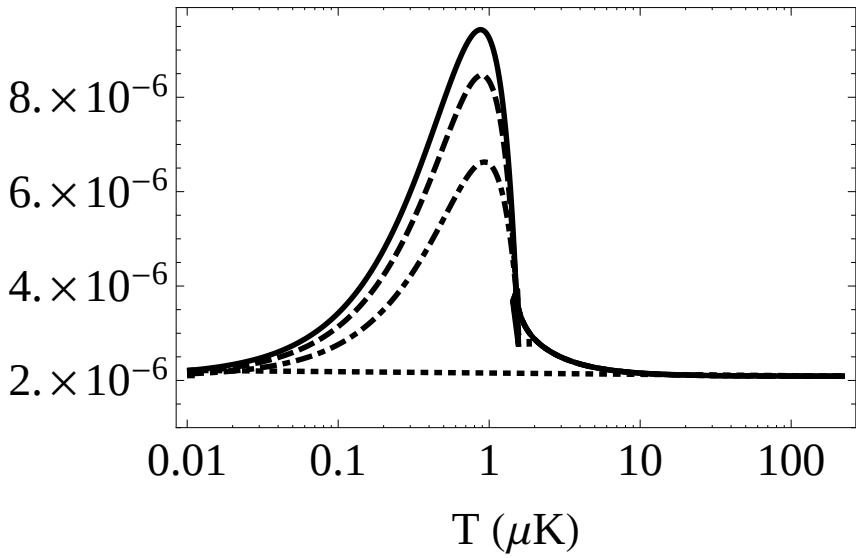

Figure 8: In this figure the imaginary part of the polarizability α is drawn as function of T with log-linear axes. This is calculated for $\lambda = 589$nm, $\delta = -4 \cdot 86.5$MHz, $\gamma = 9.79$MHz and $\rho_0 = 10^{20}\text{m}^{-3}$. The dotted line is the value without the enhancement. The dot-dashed is the value after integrating up to 0.001mm and the dashed line is the value after integrating 0.01mm. We ignored that the oscillating part isn't fully converged, so the last part of a period can give a significant contribution. The solid line is polarizability with the relative enhancement of the scattering rate integrated up to ∞.

5 Experimental results

To confirm theory, experimental results with sufficiently small uncertainties are needed. In this section the results will be described. In Section 5.1 we will describe the characteristics of the behavior of our measurements, containing of a 100 images of one single cloud. In Section 5.2 the results are summarized. In Section 5.3 some difficulties and uncertainties are described before we describe also how the measuring could be more accurate. Finally we find the results of [1] agreeing with additional effects in the theory in Section 5.4.

5.1 Some measurements of the particle number and temperature

In this section the result are shown and analyzed. The series here considered, had the pictures taken rapidly after one another (with a time between shots between 5ms and 10ms), and the mirrors were placed poorly giving a low η, and the Pre-Amplifier-Gain is 3.8. We measured the trap frequencies to be 2π 89.9Hz and 2π 15.1Hz. All the measurements in this part are in directory 20140404, though some were taken during different days.

	#	<N>	g	g_{theory}	ΔT/shot	ΔT_{theory}/shot
●	321	3103	0.023(3)	0.0345	0.037(6)	0.0432
●	295	1403	0.0118(13)	0.01559	0.026(3)	0.0195
●	338	334	0.0032(6)	0.00371	0.0014(22)	0.00465

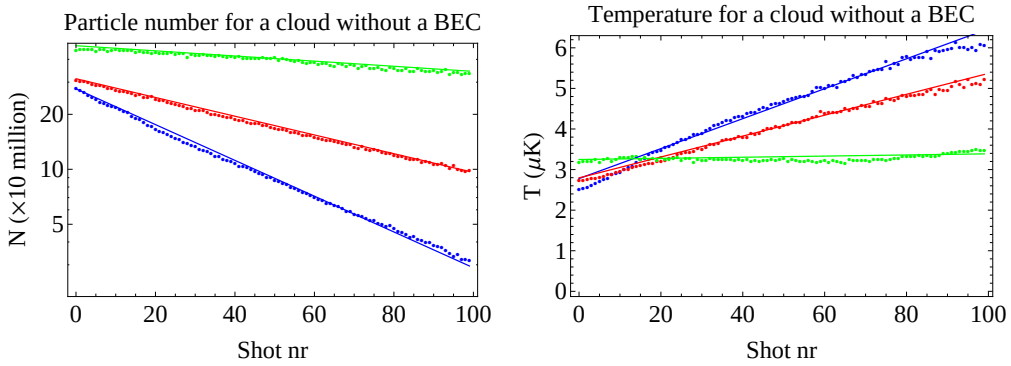

(a) (b)

Figure 9: Examples of the temperature and particle number dynamics for clouds without a BEC. Different colors represent different series with a different intensity of the probe laser, scales with $< \mathcal{N} >$. In (a) the total number of particles is shown as a function of the shot number for a cloud without a BEC. The particles are lost exponentially, as predicted, though with a exponent smaller than theory predicts. In (b) the temperature is shown as a function of the shot number. The red and the blue line seem to flatten out at the end, which is explained by the system leaving the hydrodynamic regime where particles no longer trapped don't redistribute their gained energy anymore. The green curves seems to behave rather odd, some periodic behavior in the temperature. This is explained by noise due to the use of little light. This isn't physical behavior.

In Figure 9a the number of particles is shown for three cloud without a BEC, and the corresponding temperature is shown in Figure 9b. In Figure 10a and Figure 10b the number of particles and the corresponding temperature are shown for three clouds starting with a BEC. The frames with a BEC are denoted with a '+' and the frames without a BEC are denoted with a '•'.

	#	<N>	g_{BEC}	$g_{thermal}$	g_{theory}	$\Delta T_{thermal}$/shot	ΔT_{theory}/shot
●	309	1159	0.024(4)	0.0096(10)	0.01287	0.0193(21)	0.0161
●	317	1004	0.021(3)	0.0080(9)	0.01115	0.0196(21)	0.014
●	344	327	0.0057(7)	0.0019(4)	0.003632	0.0103(11)	0.00455

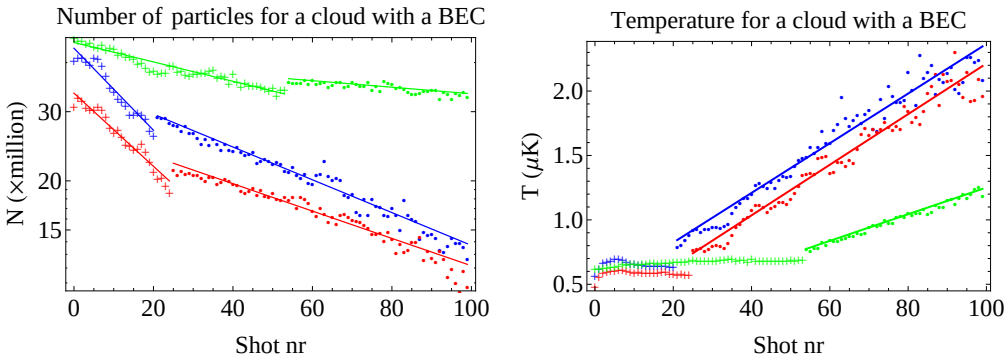

(a) (b)

Figure 10: All these figures are clouds started with a BEC. After some frames the BEC is destroyed completely. The frames with a BEC are denoted with a '+'; the frames without a BEC are denoted with a '•'. Different colors represent different series with a different intensity of the laser, that scales with $< \mathcal{N} >$. The discontinuities in the plots, where the BEC disappears completely is caused by fitting errors due to atoms no longer trapped still present. In (a) the total number of particles is shown as a function of the shot number for a cloud started with a BEC. When the BEC disappears the exponent changes. The change in exponent can be explained by the enhanced scattering rate, which can give up to a factor 3 in the exponent for a BEC. In (b) the temperature is shown as a function of the shot number for a cloud started with a BEC. For the part without a BEC the system heats up as thermal clouds who didn't start with a BEC. The decrease in temperature in the BEC could be explained by thermalization of condensed particles.

The number of particles decreases exponentially, as predicted for a constant enhancement in the scattering rate. For a cloud without a BEC there is no enhancement. For a cloud with a BEC we assume the enhancement and fraction of particles lost to be constant. For the frames with a BEC the number of particles decreases faster as predicted by the enhanced scattering rate, causing a higher exponent. The results are quantified in Section 5.2.

In the measurements without a BEC, the temperature increases in the first part linearly before the slope reduces. We expect the temperature difference per frame to satisfy $3k_B\Delta T = E_{pp}$ for $T \gg T_c$. The reduction of the slope occurs gradually and continuously. It occurs when the temperature is increased and the particle number is reduced, causing a lower density (up to a factor 10). This can be explained by leaving the hydrodynamic regime. We enter gradually the regime where the gained momentum of particles no longer

trapped isn't redistributed over the rest of the cloud. We haven't quantified this.

Even though we made a prediction for the energy per particle and temperature for a cloud with a BEC, we won't compare theory and experimental results. The enhancement isn't constant and isn't experimentally well enough determined. Also the change in energy per particle is small for a cloud with a BEC, compared to the statistic and systematic errors.

Both in the temperature and in the number of particles there is a discontinuity when the BEC is no longer detected. A discontinuity isn't physical behavior. There seems to be also some start-up effect in the first 5 frames when there is a BEC (temperature increase and the lack of losing particles). This will be described in Section 5.3.

5.2 Quantifying the results

Here the results are quantified. The temperature difference per frame is plotted against the average pixel count $< \mathcal{N} > \propto I_{laser}$ in Figure 11a. Under these circumstances the background effects were measured to be up to 0.001μK per frame. However there seems to be some kind of cutoff of approximately 0.008μK per frame. We found that the experimental results over the theoretical results $\frac{E_{pp,\text{experiment}}}{E_{pp,\text{theory}}}$ varies from 0.9 up to 2.2, caused by the cutoff. If we include a cutoff, vary those from 0.7 up to 1.2. In both cases we excluded some measurements (20%) with the worst noise (like the green curve in Figure 9b).

In Figure 11b the exponent of the particle loss is given as a function of the number of counts per pixel, including a theoretical prediction. Background effects for a cloud without a BEC with little time between shots appear to be negligible. However the exponent divided by the counts $g/\mathcal{N}$ seems to decrease when more light is used. The experimental results over the theoretical results $\frac{g_{\text{experiment}}}{g_{\text{theory}}}$ vary from 0.65 up to 0.95, depending on the amount of light.

The fraction of particles is lost when there is a BEC, is on average 2.6(3) times higher than when there isn't a BEC. When there was a BEC in measurement 309 the average value for the chemical potential was $\mu \approx 2.3$kHz and temperature of $T \approx 0.66\mu$K. For the measurement 317 and 344 the conditions were similar. Comparing this with our theoretical prediction in Figure 7, we expect an enhancement of a factor 2.0. So our measurements are within two times the uncertainty. Since the chemical potential and temperature change over the frames we expect the enhancement to change as well. We couldn't measure accurate enough to get experimental a frame to frame enhancement.

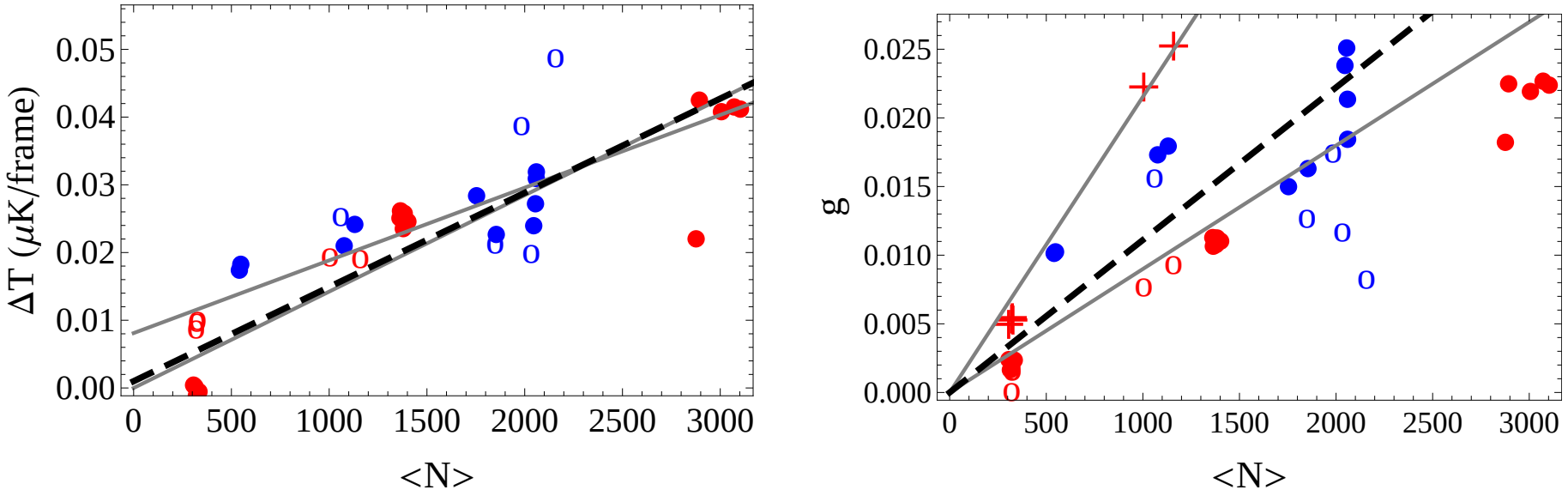

(a) (b)

Figure 11: The values for the series started without a BEC are denoted with a '•', those with a BEC with a '+' and when the BEC is destroyed with a 'o'. The dotted lines are the theoretical values (we didn't include an extra cutoff effect). The solid gray lines is the average experimental value. The different colors are measurements of two different days. In (a) the temperature increase per frame is shown as a function of the pixel count $\mathcal{N}$. The best linear regressions, with and without offset, are drawn. There seems to be some kind of cutoff, some temperature increase will occur even without any laser light, though this was measured directly to be negligible ($<0.001\mu$K) for the red measurements (we didn't measure the background effects for the black measurements). In (b) the exponent of the particle loss is shown as a function of the pixel count $\mathcal{N}$. The best linear regressions without an offset are drawn the thermal clouds '•','o' and the clouds with a BEC '+'. For a cloud with a BEC, where the conditions as temperature and chemical potential are similar, the slope of the exponent versus the pixel count is a lot steeper than for the cloud without a BEC. If the conditions of the BEC are different, different slopes are expected.

5.3 Difficulties, uncertainties and improvements for future measurements

In Figure 10 discontinuities were detected when the BEC is no longer detected. There seems to be also some start-up effect in the first 5 frames when there is a BEC (temperature increase and the lack of losing particles). This is caused by the failure of our fit. We have noticed a BEC still present when the BEC is no longer detected by our fit. The failure of our fit is explained by particles no longer trapped still present. Those particles will change the shape of our cloud. After $\sim$20 frames when the BEC is no longer detected the BEC is really destroyed, and the fit is correct again. The failure of the fit those $\sim$20 frames cause the discontinuity. The particles no longer trapped still present may also cause some startup effects, like the increase in temperature and the lack of losing particles in the first 5 frames when there is a BEC present.

The effect of the particles no longer trapped still present will give a too high energy increase since the cloud becomes wider $\rightarrow$ increased temperature and a to low fraction of particles lost since the particles are still present. We haven't quantified this.

The startup effect and the failure of the fit are caused by taking the two shots rapidly after one another, our model fails to fit some images due to atoms not longer trapped still present. This effect is extremely important when there is a BEC (due to high densities and collision rates). Atoms no longer trapped but still present, may also play a role for clouds without a BEC. This effect increases when there is a lot of light in one shot. Using little light is not desirable, the images get noisy and hard to analyze.

Increasing the time between two shots introduced new problems. We found that the effect we were looking for (heating up of particles and losing particles due to the light), would be small compared to background effects when there is little light or a lot of time between shots (effects due to impurities of the trap, impurities of the vacuum). To make matter worse, the background effects seemed to depend on the size and temperature of the cloud, causing the background effect not to be constant and hard to compensate.

Despite these difficulties we think we have the ingredients to analyze more accurate than [1], due to the use of more light (less noise in the pictures) and placement of the camera such that the BEC is on a spot where there are minimal interference effects in the background. We see less noise in the measured temperature and number of particles. However reducing the effects of particles lost but still in the trap or subtracting the background heating and loss is a challenge.

A difficulty we couldn't solve was the phase spot in our PCI setup. We used a phase spot with $\theta = \pi/3 \approx 1.047$, so we expected a relative intensity I/I_0 for the background of 1, and for the atoms periodic between $0 \leq I/I_0 \leq 4$. Unfortunately, even after different ways of aligning the system correctly, we got a relative intensity up to 5.0 ± 0.4, with $5.0 > 4$. By using a slightly bigger phase spot $\theta = 1.3$ we expect a relative intensity up to 5.0, but the shape of our model of an image of the cloud doesn't seem to be improving, and due to some noise and day to day miss aligning effects, we have quite some uncertainty for our maximum relative intensity, so we still use in our calculations a phase spot of $\theta = \pi/3$. In this thesis we try to measure the particle number decrease and

the temperature change. We have calculated those for different phase spots and found for a cloud without a BEC no difference ($< 2\%$) and for a cloud with a BEC only a small difference ($\sim 20\%$).

Here I will summarize how the noise and uncertainties can be reduced in the measurements. The aligning should be optimized before the measurements, and during the measurements the background light should be minimized. Using a high intensity of the light on the camera will noise, as well as placing the camera such that there are no interference effects in the background image at the BEC. Fixing the center and using SVD in our analyzes reduces also noise.

An optimum should be found for the time between shots, large enough to let atoms no longer trapped escape though not to large to keep background effects minimal compared to the scattering effects. Using a high intensity of light at the atoms will increase the effects of scattering. To prevent the camera overexposing a filter should be placed in the light beam before the camera. During the fit we can first fit the temperature on the thermal part of the cloud containing a BEC (ignoring the atoms no longer trapped still present in the high densities of the BEC), before we determine the chemical potential with a fixed temperature.

It is necessary to understand the phase spot better to explain the signal which goes to a value larger than expected. A possibility is to determine the maximum average value of the signal I/I_0 in measurements with a BEC and no noise and experimentally obtain a value for the size of the phase spot.

5.4 Results of Damaz de Jong for a cloud without a BEC

Since my thesis uses the results of Damaz de Jong [1, Sec 5.2], I will also describe his results. He found for a cloud without a BEC experimentally $g/\mathcal{N} = 25.2(7) \times 10^{-6}$ and $E_{pp}/\mathcal{N} = 97(4)$pK. He concluded that these results were a factor 5 and a factor 16 higher than he predicted.

I have included the following additional effects in his theory: an coefficient η for the loss of light, assuming the cloud is in the hydrodynamic regime, and a slightly different value for the average energy transfer. I can make new theoretical predictions with a 10% uncertainty due to the accuracy of the measurement of η, for losses of light due to our mirrors. Theory predicts $\bar{g}/\mathcal{N} = 29(3) \times 10^{-6}$ and $\bar{E}_{pp}/\mathcal{N} = 107(10)$pK. For both the energy as the particle number we find our theoretical value approximately 10% too high. We think it would be plausible that our value for η could have changed during the year. Even ignoring a possible change in η, theory and experiment are within two times the standard deviation. So we can conclude that with some additional theory, experimental results of [1, Sec 5.2] and theoretical predictions coincide.

6 Conclusion

In this thesis we have considered the scattering rate, when near resonant light beam illuminates a cloud of cold atoms. By illumination we lose particles and we add energy to the system. We have got a better understanding of the scattering of particles and the background effects.

For the case without a BEC we have the following conclusions about particle loss and energy increase. We found that theory and experiment differ at most 30%. We had problems with atoms no longer trapped to remain present, which can be solved by waiting longer between shots, though not to long too make background effects significant. We think we can decrease the uncertainties in our measurements. We could conclude that with some additional theory as written in Section 5.4, the experiment of [1] agrees with theory for a cloud without a BEC.

For the case with a BEC an enhancement in the scattering rate was calculated, due to effects of neighboring atoms on the polarizability. This enhanced scattering was measured in the particle loss and was within the uncertainty of our calculation. Though we had to approximate that during a some shots the temperature and chemical potential were constant. This approximation was necessary since our measurements were too noisy. For the energy of the system we couldn't compare theory and experiment, because we have too much uncertainties in our measurements, in the enhancement and the determining of the temperature and chemical potential.

Acknowledgements

Research and results are often the result of collaboration, including my research. For this collaboration I would like to thank all the staff of the Debye Institute of the group Atom Optics and Ultra-fast Dynamics. Explicitly I first would like to thank my supervisor prof. dr. Peter van der Straten, not only for giving me the opportunity to do research in his group, but mostly for helping me out when I got stuck in the theory, listening to my speculations how theory might explain results and correcting me when these speculations were wrong. I would like to thank Pieter Bons, PhD student in my group, for providing me with the experimental data and helping me to get an interpretation of some articles and scripts. Further more I would thank Damaz de Jong, who did his bachelor research a year before me, for providing me a research topic, some help to get started and enough open ends.

Martijn van 't Woud, Johan van der Toll, Peter Elroy and Alexander Groot are appreciated for introduced me to their research, showing the possibilities of our experimental setup when I started my research. I also appreciate the conversations about our researches I had with Michel Ram, Maxim Faber, Christian te Riet and Thijs van Gogh. Here some new concepts were introduced and often rejected by pointing out the weak points with the concepts, but also the conversation without any relevance to physics.

References

[1] D. de Jong. *Specific Heat of an Ultracold Bose Gas in a Harmonic Trap.* Bachelor Thesis, 2013

[2] R. Meppelink. *Hydrodynamic excitations in a Bose-Einstein condensate.* PhD thesis, Universiteit Utrecht, 2009.

[3] Olivier Morice, Yvan Castin, and Jean Dalibard. *Refractive index of a dilute Bose gas.* Phys. Rev. A 51, 3896, 1994

[4] O. Morice. *Atomes refroudis par laser: du refroidissement sub-recul à la recherche d'effets quantiques collectifs.* Thèse de doctorat de l'université Paris VI, 1995

[5] C.J. Pethick and H. Smith. *Bose-Einstein Condensation in Dilute Gases.* Cambridge University Press, 2002.

[6] Jasper Smits. *Formation of Faraday patterns in cigar-shaped Bose-Einstein condensates.* Bachelor Thesis, 2013.

[7] Harold J. Metcalf and Peter van der Straten. *Laser cooling and trapping.* Springer, 1999.

[8] Lincoln D. Turner, Karl P. Weber, David Paganin, and Robert E. Scholten. *Off-resonant defocus-contrast imaging of cold atoms* 2004

[9] P. J. Ungar, D. S. Weiss, E. Riis, and Steven Chu. *Optical molasses and multilevel atoms: theory* 1989

[10] Daniel A. Steck. Sodium D Line Data 2000